ELSEVIER

www.elsevier.nl/locate/jorganchem

Journal of Organometallic Chemistry 592 (1999) 46–51

Journal of Organometallic Chemistry

Isolation of pentamethylcyclopentadienyl tris(*tert*-butylthiolato) complexes of tungsten(IV) and carbon–sulfur bond activation

Takayuki Nagasawa [a], Hiroyuki Kawaguchi [b], Kazuyuki Tatsumi [a,*]

[a] *Research Center for Materials Science, and Department of Chemistry, Graduate School of Science, Nagoya University, Furo-cho, Chikusa-ku, Nagoya 464-8602, Japan*

[b] *Coordination Chemistry Laboratories, Institute for Molecular Science, Myodaiji, Okazaki 444-8595, Japan*

Accepted in revised form 5 August 1999

Abstract

A thermally unstable *tert*-butylthiolato complex of tungsten (IV), Cp*W(S^{t}Bu)$_3$ (**1**), was isolated from the reaction between Cp*WCl$_4$ and four equivalents of LiS^{t}Bu in THF at −78°C. Degradation of **1** occurred in solution at room temperature via C–S bond cleaving reactions to generate a complex mixture containing Cp*W(S)$_2$(S^{t}Bu) (**2**), *anti*-Cp*$_2$W$_2$(S)$_2$(μ-S)$_2$ (**3**), and *syn*-Cp*$_2$W$_2$(S)$_2$(μ-S)$_2$ (**4**). Complex **1** was converted into a thermally stable ^{t}BuNC adduct, Cp*W(S^{t}Bu)$_3$(CN^{t}Bu) (**5**), which was also obtained from the Cp*WCl$_4$/LiS^{t}Bu/CN^{t}Bu reaction system. Compounds **1**, **4**, and **5** have been structurally characterized by X–ray diffraction. © 1999 Elsevier Science S.A. All rights reserved.

Keywords: Tungsten; Thiolato complex; Isocyanide complex; Carbon–sulfur bond activation

1. Introduction

We recently reported that the reactions of Cp*MoCl$_4$ or Cp*WCl$_4$ with lithium salts of *tert*-butylthiolato and 1,2-ethanedithiolato gave rise to a variety of mononuclear molybdenum or tungsten thiolato/sulfido complexes carrying a pentamethylcyclopentadienyl auxiliary ligand [1]. For instance, the treatment of Cp*WCl$_4$ with Li$_2$edt (edt = SCH$_2$CH$_2$S) in THF at room temperature followed by a cation exchange reaction with PPh$_4$Br in CH$_3$CN afforded (PPh$_4$)[Cp*W(S)$_3$] in high yield. An analogous reaction between Cp*WCl$_4$ and LiS^{t}Bu generated Cp*W(S)$_2$(S^{t}Bu) and *anti*-Cp*$_2$W$_2$(S)$_2$(μ-S)$_2$. In these reactions, C–S bond cleavage took place with concomitant oxidation of the tungsten atom from W(V) to W(VI). In contrast, the reactions of the molybdenum congener Cp*MoCl$_4$ with Li$_2$edt and LiS^{t}Bu gave rise to (PPh$_4$)[Cp*Mo(edt)$_2$] and Cp*Mo(S^{t}Bu)$_3$, respectively, where the molybdenum atom was reduced from Mo(V) to Mo(IV). Occurrence of the reduction for the molybdenum system is not surprising under the presence of lithium thiolates, because they may act as reducing reagents [2]. On the other hand C–S bond cleavage might have induced oxidation of the tungsten system, or the tendency of tungsten favor high oxidation states might have promoted the C–S bond activation.

The synthesis of the Mo(IV) thiolato complexes lead us to presume that the analogous W(IV) thiolato complexes could be formed prior to C–S bond cleaving reactions. Our efforts to examine such possibility resulted in isolation of Cp*W(S^{t}Bu)$_3$ (**1**) at low temperature from the reaction of Cp*WCl$_4$ with LiS^{t}Bu. Complex **1** was found to be transformed to a thermally stable form, Cp*W(S^{t}Bu)$_3$(CN^{t}Bu) (**5**), by addition of ^{t}BuNC to **1**. In this paper, we report the synthesis and characterization of **1** and **5**, and the thermal degradation of **1** at room temperature in C$_6$D$_6$.

2. Results and discussion

Addition of four equivalents of LiS^{t}Bu to Cp*WCl$_4$ in THF at −78 C yielded a red solution. Quick removal of the solvent left a red powder, which was crystallized from HDMSO at −30°C to give analytically pure Cp*W(S^{t}Bu)$_3$ (**1**) in 56% yield. The modest isolated yield is partly due to the high solubility of **1** in hydro-

* Corresponding author.

PII: S0022-328X(99)00478-7

carbon solvents. The ^{1}H-NMR spectrum of **1** in C_6D_6 displays two singlets at δ 2.11 and 1.88 for the Cp* and ^{t}Bu groups, respectively, in an intensity ratio of 5:9. From this reaction, ^{t}BuSS^{t}Bu was detected as a byproduct by GC/MS analysis, indicating that one equivalent of LiS^{t}Bu is consumed to reduce the tungsten atom from W(V) to W(IV). The X-ray analysis of **1** revealed that the molecule assumes a pseudotetrahedral arrangement at tungsten with one Cp* ring and three sulfurs. The molecular structure is presented in Fig. 1, and selected bond distances and angles are listed in Table 1. The crystal of **1** is isomorphous to that of the molybdenum analogue Cp*Mo(S^{t}Bu)$_3$, and their geometrical parameters are similar [1a]. The W–S distances fall within a normal range [3,4], and the average W–S distance is longer than that of W(S^{t}Bu)$_4$ (2.236(4) Å) [5] (Scheme 1).

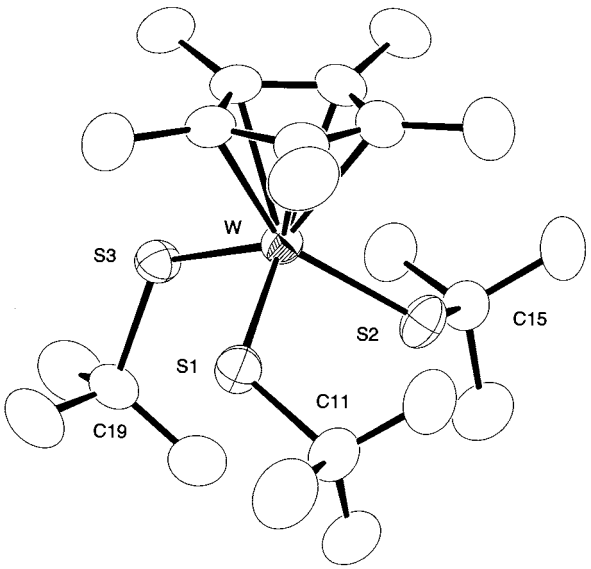

Fig. 1. Molecular structure of Cp*W(S^{t}Bu)$_3$ (**1**).

Table 1
Selected bond distances (Å) and angles (°) for Cp*W(S^{t}Bu)$_3$ (**1**) and Cp*W(S^{t}Bu)$_3$(CN^{t}Bu) (**5**)

	1	**5**
Bond lengths		
W–S1	2.329(1)	2.381(3)
W–S2	2.297(1)	2.458(3)
W–S3	2.263(1)	2.338(3)
W–C23		2.05(1)
C23–N		1.17(1)
Bond angles		
S1–W–S2	94.31(5)	84.7(1)
S1–W–S3	98.82(5)	121.1(1)
S2–W–S3	110.84(5)	85.6(1)
S1–W–C23		70.6(3)
S2–W–C23		148.0(3)
S3–W–C23		90.0(3)
W–S1–C11	121.8(2)	129.5(4)
W–S2–C15	119.9(2)	124.9(4)
W–S3–C19	122.1(2)	123.7(4)
W–C23–N		175.3(9)
C23–N–C24		164(1)
Cp*–W–S1	110.4	119.8
Cp*–W–S2	119.1	108.1
Cp*–W–S3	118.4	118.4
Cp*–W–C23		102.1
Cp*–W–S1–C11	96.8	123.4
Cp*–W–S2–C15	97.1	99.5
Cp*–W–S3–C19	160.3	104.5

Although **1** is relatively stable as a solid under argon atmosphere, it is thermally unstable in solution. For instance, complex **1** decomposes in C_6D_6 with a half-life of ca. 1.5 h at 25°C, according to the ^{1}H-NMR spectroscopy. The degradation of **1**, associated with C–S bond cleavage, appears to occur in a complicated fashion. At an early stage of the degradation, the NMR spectrum shows new resonances arising from Cp*W(S)$_2$(S^{t}Bu) (**2**), *anti*-Cp*$_2$W$_2$(S)$_2$(μ-S)$_2$ (**3**), and *syn*-Cp*$_2$W$_2$(S)$_2$(μ-S)$_2$ (**4**), and some unassignable signals appear as well in the 1.6–2.2 ppm region in addition to the signals of organic byproducts. However, eventually the spectrum becomes dominated by the resonances of **3** and **4** with an intensity ratio of ca. 8:1. The GC–MS analysis of the organic byproducts revealed the formation of ^{t}BuS^{t}Bu, ^{t}BuSS^{t}Bu, and isobutene.

We examined the degradation reaction of **1** in a preparative scale. Thus a red THF solution of **1** was stirred for 1 h at room temperature. Isolation of products from this solution was not easy, and the extraction and recrystallization of the crude product from hexane and then from toluene barely allowed us to obtain **2** and **3** in 24 and 14% yields, respectively. When a THF solution of **1** was stirred for 12 h, the color of the solution became brown. In this case, we applied a chromatographic separation of the products on a silica gel column eluting with toluene, from which **3** (68%) and a small amount of **4** (4%) were isolated. We previously reported the synthesis and X-ray structures of **2** and **3** [1a]. Complex **4** was identified by the spectroscopic data, combustion analysis, and eventually the structure was determined by X-ray diffraction. The molecular structure of **4** is presented in Fig. 2, and selected bond distances and angles are given in Table 2. The X-ray-derived structure of a closely related dinuclear complex, *syn*-(C$_5$Me$_4$Et)$_2$W$_2$(S)$_2$(μ–S)$_2$, is known, and its structural feature and the metric parameters are practically identical to those of **4** [6]. In the structure of **4**, the W$_2$(μ–S)$_2$ ring is puckered with a dihedral angle of 22° between the W1W2S1 and W1W2S2 planes. The two terminal sulfido ligands are arranged in a *syn* configuration, and the S3–W1–W2–S4 twist angle is 2.2(1)°. The W1–W2 distance of 2.8785(5) Å indicates the presence of a metal–metal single bond between the two d^1 W(V) centers, and the observed distance is

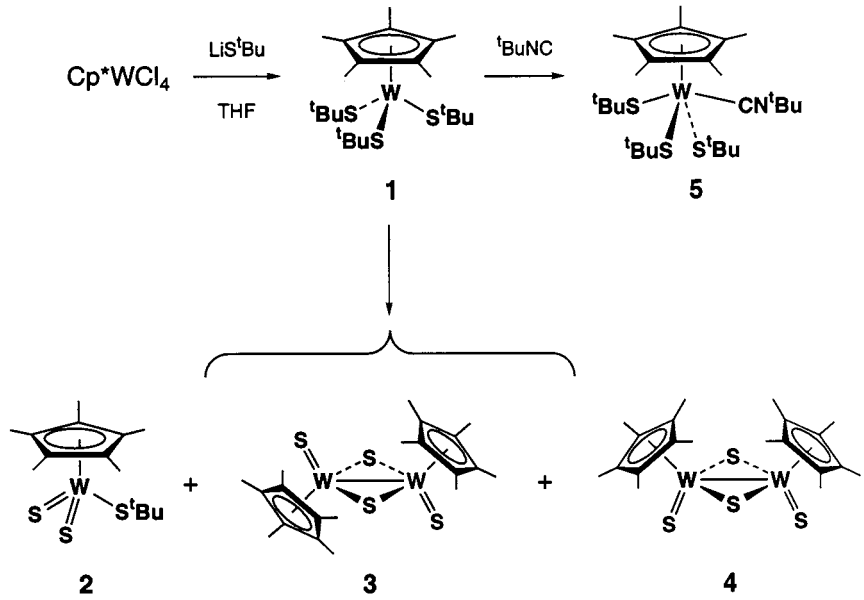

Scheme 1.

somewhat shorter than that of the *anti*-isomer **3** (2.900(1) Å) [7].

Thermal instability of the monomeric W(IV) thiolato complex **1** in solution contrasts with the behavior of the analogous molybdenum complex Cp*Mo(S^{t}Bu)$_3$ which is stable both in solid and in solution at room temperature for a prolonged period in the absence of air/water [1a]. Degradation of **1** takes place with C–S bond cleavage reactions of the thiolate, and with concomitant oxidation of tungsten. Although the cause of the degradation is not clear at the moment, the different thermal stability between the W(IV) and Mo(IV) thiolate complexes might arise from the tendency of tungsten to favor higher oxidation states compared with molybdenum. One way to stabilize the W(IV) thiolate complex would be to introduce an electron-withdrawing ligand at the metal center. In fact, a CO adduct of the analogous thiolate complex, (η^5-C$_5$H$_5$)W(SC$_6$F$_5$)$_3$(CO) [3], has been reported, where the C–S bond of thiolate itself is also stabilized by a strongly electron-withdrawing substituent. Our attempt to react **1** with 1 atm CO failed, because **1** was transformed into **2** and **3** before it reacted with CO. However, the reaction of **1** with one equivalent of ^{t}BuNC in toluene smoothly proceeded to afford Cp*W(S^{t}Bu)$_3$(CN^{t}Bu) (**5**) in 90% isolated yield. In this reaction, the oxidation state of the tungsten is retained as W(IV). We note here that the reaction of Cp*Mo(S^{t}Bu)$_3$ with ^{t}BuNC turned out to induce further reduction of molybdenum to Mo(II), giving rise to Cp*Mo(S^{t}Bu)(CN^{t}Bu)$_3$ [8].

The isocyanide adduct **5** is in fact thermally stable, and does not show any sign of decomposition in C$_6$D$_6$ at room temperature for 1 week, according to its ^{1}H-NMR spectrum. The spectrum consists of sharp singlets at 1.68, 1.64, and 1.62 ppm with an intensity ratio of 1:2:1, which are assigned to the *tert*-butyl groups, and the resonance of Cp* at 2.03 ppm. The IR spectrum of **5** exhibits a strong absorption band at 2060 cm^{-1} assignable to the N≡C stretching vibration. This band is

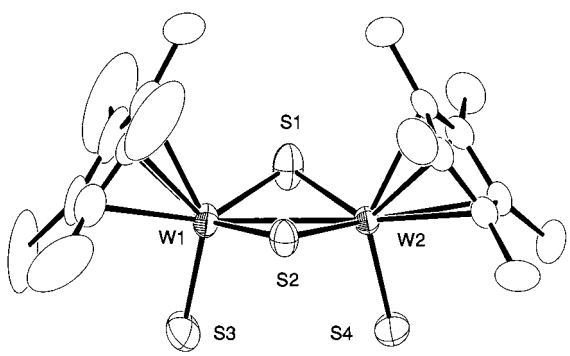

Fig. 2. Molecular structure of *syn*-Cp$^*_2$W$_2$(S)$_2$(μ-S)$_2$ (**4**).

Table 2
Selected bond distances (Å) and angles (°) for *syn*-Cp$^*_2$W$_2$(S)$_2$(μ-S)$_2$ (**4**)

Bond lengths			
W1–W2	2.8785(5)	W2–S1	2.304(2)
W1–S1	2.310(3)	W2–S2	2.300(2)
W1–S2	2.303(2)	W2–S4	2.149(3)
W1–S3	2.154(3)		
Bond angles			
S1–W1–S2	99.95(8)	S1–W2–S2	100.20(9)
S1–W1–S3	107.1(1)	S1–W2–S4	105.4(1)
S2–W1–S3	104.3(1)	S2–W2–S4	106.1(1)
S3–W1–W2	101.48(8)	S4–W2–W1	101.58(8)
W1–S1–W2	77.19(8)	W1–S2–W2	77.42(8)

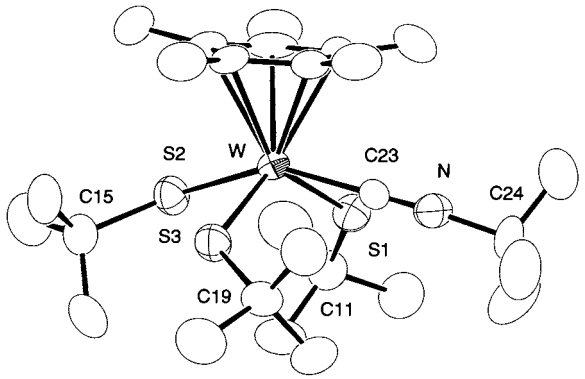

Fig. 3. Molecular structure of Cp*W(S^{t}Bu)$_3$(CN^{t}Bu) (**5**).

largely shifted to a lower frequency compared with the corresponding IR band of free ^{t}BuNC (2145 cm^{-1}), and it is also much lower than the N≡C bands found for the related W(IV) complexes [(η^5-C_5H_5)$_2$W(CNR)Cl](PF$_6$) (R = ^{t}Bu, 2207, 2192 cm^{-1}; Et, 2178 cm^{-1}) [9]. This observation indicates that strong π back-donation to the isocyanide occurs in **5**, and in turn explains the tendency of **1** to be readily oxidized, being without coordination of isocyanide.

The molecular structure of **5**, shown in Fig. 3, was determined by X-ray diffraction. Selected bond distances and angles are compared with those of **1** in Table 1. Complex **5** adopts a distorted four-legged piano-stool structure, where the S1–W–S3 angle is notably smaller than the S2–W–C23 angle. Below the Cp* ligand, the *tert*-butyl groups of S^{t}Bu are bent in the same direction. All the S–C vectors tend to be parallel to the Cp* plane, where the Cp*–W–S–C torsion angles vary from 99.5 to 123.4°. Four-legged piano-stool structures put two d orbitals at low energies, namely d_{z^2} and d_{xy} [10]. In the low-spin d^2 electronic configuration, two electrons should reside in one of the two d orbitals leaving the other unoccupied. Considering the observed orientation of the *tert*-butyl groups of thiolates, d_{z^2} orbital must be designated as unoccupied, because the occupied π orbital of each S atom is situated so as to overlap well with d_{z^2} and to donate electrons. On the other hand, the occupied d_{xy} back-donates electrons to a π* orbital of CN^{t}Bu. The W–C23–N–C24 spine is essentially linear with the C23–N bond distance of 1.17(1) Å, and the W–C23 distance of 2.05(1) Å is comparable to that of [(η^5-C_5H_5)$_2$WCl(CNEt)](PF$_6$) (2.036(10) Å). The average W–S distance of 2.392 Å is significantly longer than that of **1** (2.296 Å), presumably due to the steric congestion of **5**, and it is comparable to that of (η^5-C_5H_5)W(SC_6F_5)$_3$(CO) (2.386 Å) [7]. Interestingly, the W–S (S1 and S3) bonds *cis* to the isocyanide ligand are evidently shorter than the W–S2 bond. The differences amount to 0.077 Å and 0.120 Å. We interpret this trend in terms of larger Cp*–W–S angles for the thiolates *cis* to the isocyanide, which would permit better π interactions. Successful isolation of **5**, which is much easier to handle than **1**, will allow us to examine reactions of the W(IV) thiolate in more detail, and to use it as a convenient precursor for synthesis of sulfido complexes.

3. Experimental

All reactions were carried out using standard Schlenk techniques under an argon atmosphere. Solvents were pre-dried and refluxed over the appropriate drying reagents under argon and collected by distillation before use. Compound Cp*WCl$_4$ was prepared as reported [11], while ^{t}BuSH and ^{t}BuNC were obtained from commercial sources and were used as received. ^{1}H-NMR spectra were recorded on a Varian Unity plus–500 spectrometer at ambient temperature. For UV–vis spectra, a Jasco V–560 spectrometer was used. Infrared spectra were recorded on Parkin–Elmer 2000FT–IR and Jasco A–3 spectrometers. Mass spectra were collected on a Shimazu QP5000 mass spectrometer. Elemental analyses were performed on a LECO-CHNS microanalyzer where the crystalline samples were sealed in thin silver tubes.

3.1. Synthesis of Cp*W(S^{t}Bu)$_3$ (1)

Addition of a THF (20 ml) solution of LiS^{t}Bu (8.87 mmol) to a slurry of Cp*WCl$_4$ (1.01 g, 2.19 mmol) in THF (20 ml) at −78°C formed a red homogeneous solution, and the solvent was immediately removed in vacuo. The residue was extracted with hexamethyldisiloxane (HMDSO) and centrifuged to remove LiCl. Concentration of the supernatant and the subsequent cooling to −30°C resulted in deposition of **1** as red plates (0.72 g, 56%). ^{1}H-NMR (C_6D_6): δ 2.11 (s, 15H, C_5Me_5), 1.88 (s. 27H, $SCMe_3$). IR (Nujol mull/KBr): 1384 s, 1372 s, 1358 s, 1269 m, 1165 s, 1128 s cm^{-1}. MS (EI): *m*/*z* 472 (M^+–2CMe_3), 415 (Cp*WS_3H^+), 383 (Cp*WS_2H^+). UV–vis (λ_{max}, nm (ε, M^{-1} cm^{-1}), hexane): 460 (sh), 420 (1100), 512 (920). Anal. Calc. for $C_{22}H_{42}S_3W$: C, 45.04; H, 7.22; S, 16.40. Found: C, 45.41; H, 7.35; S, 16.91.

3.2. Degradation of 1 into tungsten sulfido complexes

3.2.1. Stirring of a THF solution of 1 for 1 h

A THF (10 ml) solution of **1** (0.48 g, 0.82 mmol) was stirred for 1 h at room temperature (r.t.). The red solution gradually darkened. After removal of the solvent, the residue was extracted with hexane (10 ml) to leave a brown solid. Concentration of the hexane solution and cooling to −30°C gave Cp*W(S)$_2$(S^{t}Bu) (**2**) as red crystals in 24% yield (93 mg). The brown residue was crystallized from toluene to give *anti*-Cp*$_2$W$_2$(S)$_2$(μ-S)$_2$ (**3**) (45 mg, 14%).

3.2.2. Stirring of a THF solution of **1** for 12 h

When a solution of **1** (0.92 g, 1.57 mmol) in THF (20 ml) was stirred for 12 h at r.t., the color of the solution turned eventually to brown. The solvent was removed under vacuum to leave a brown solid, which was purified by chromatography on a silica gel column eluting with toluene. From the first reddish–brown band, 0.41 g of **3** was obtained (68%). On the other hand, the second brown band gave 0.024 g of *syn*-$Cp^*_2W_2(S)_2(\mu\text{-}S)_2$ (**4**) (4%). Data for **4:** ^{1}H-NMR ($CDCl_3$): δ 2.21 (s, C_5Me_5). IR (Nujol mull/KBr): 482 s, 470 m cm^{-1}. Anal. Calc. for $C_{20}H_{30}S_4W_2$: C, 31.34; H, 3.95; S, 16.74. Found: C, 30.40; H, 3.99; S, 16.11.

3.3. Synthesis of $Cp^*W(S^tBu)_3(CN^tBu)$ (**5**)

3.3.1. Method A

Compound **1** (0.89 g, 1.52 mmol) was dissolved in 30 ml of toluene at −78°C to produce a red solution. To this stirred solution was added 0.21 ml of ^{t}BuNC (1.86 mmol). The solution immediately turned bright red. The solution was evaporated under vacuum to leave a red solid. The resulting residue was dissolved in a minimum amount of hexane and cooled to −30°C, giving rise to 0.92 g of **5** as red crystals (90%).

3.3.2. Method B

A solution of LiS^{t}Bu (5.30 mmol) in THF (20 ml) was added to a THF (20 ml) solution of Cp^*WCl_4 (0.56 g, 1.22 mmol) containing ^{t}BuNC (0.15 ml, 1.32 mmol) at −78°C. The mixture was warmed up to r.t. and stirred for 30 min. The resulting red solution was evaporated to dryness. The residue was extracted with hexane and centrifuged to remove LiCl. The hexane solution was concentrated and cooled to −30°C to afford **5** (0.64 g, 79%). ^{1}H-NMR (C_6D_6): δ 2.03 (s, 15H, C_5Me_5), 1.68 (s, 9H, CMe_3), 1.64 (s, 18H, CMe_3), 1.62 (s, 9H, CMe_3). IR (Nujol mull/KBr): 2060 (s, $\nu_{N\equiv C}$), 1358 (s), 1350 (m), 1260 (s), 1228 (w), 1205 (m), 1160 (m), 1160 (s) cm^{-1}. Anal. Calc. for $C_{27}H_{51}NS_3W$: C, 48.42; H, 7.68; N, 2.09; S, 14.36. Found: C, 48.20; H, 7.90; N, 2.07; S, 14.36.

3.4. X-ray structure determination of **1**, **4**, and **5**

Crystals of **1** and **5** suitable for X-ray analysis were mounted in glass capillaries and sealed under argon. Diffraction data were collected at r.t. on a Rigaku AFC7R diffractometer employing graphite-monochromated Mo–K_α radiation ($\lambda = 0.710690$ Å) and using the $\omega - 2\theta$ scan technique. Refined cell dimensions and their standard deviations were obtained from

Table 3
Crystallographic data for $Cp^*W(S^tBu)_3$ (**1**), *syn*-$Cp^*_2W_2(S)_2(\mu\text{-}S)_2$ (**4**), and $Cp^*W(S^tBu)_3(CN^tBu)$ (**5**)

	1	**4**	**5**
Formula	$C_{22}H_{42}S_3W$	$C_{20}H_{30}S_4W_2$	$C_{27}H_{51}S_3NW$
Molecular weight (g mol^{-1})	586.6	766.40	669.74
Crystal system	Triclinic	Tetragonal	Triclinic
Space group	$P\bar{1}$ (No. 2)	$P4_12c$ (No. 114)	$P\bar{1}$ (No. 2)
Crystal size (mm)	0.90 × 0.60 × 0.35	0.10 × 0.02 × 0.01	0.50 × 0.05 × 0.05
a (Å)	9.305(2)	23.7449(5)	10.381(3)
b (Å)	16.284(3)		18.845(7)
c (Å)	9.287(4)	8.3995(2)	9.097(3)
α (°)	92.05(2)		103.45(3)
β (°)	107.46(3)		113.71(3)
γ (°)	103.75(2)		80.54(3)
V (Å^3)	1295.2(7)	4735.8(2)	1579(1)
Z	2	8	2
ρ_{calc} (g cm^{-3})	1.504	2.150	1.408
μ (Mo–K_α) (cm^{-1})	47.11	100.75	38.73
$2\theta_{max}$ (°)	50	55	55
Abs. range	0.38–1.00	0.54–1.00	0.81–1.00
Decay (% decline)	3.43		16.33
Number of unique reflections	4552	3014	7268
Number of observations data [a,b]	4214	2488	4668
Number of parameters	235	237	289
Residuals (R/R_w) [c]	0.024/0.040	0.035/0.058	0.051/0.066
Goodness-of-fit [d]	1.68	1.57	1.50

[a] At room temperature.
[b] Observation criterion $I > 3\sigma(I)$.
[c] $R = \Sigma \| F_o | - | F_c \| / \Sigma | F_o |$. $R_w = [\{\Sigma\, w(|F_o| - |F_c|)^2\} / \Sigma\, wF_o^2]^{1/2}$.
[d] Goodness-of-fit $= [\{\Sigma\, w(| F_o | - | F_c |)^2\} / (N_o - N_p)]^{1/2}$, where N_o and N_p denote the numbers of data and parameters.

least-squares refinements of 25 randomly selected centered reflections. Three standard reflections, monitored periodically for crystal decomposition or movement. The crystals of **1** and **5** showed intensity decay (3.43% decline for **1**; 16.3% decline for **5**) over the course of the data collections. The raw intensities were corrected for the decay, and for Lorenz and polarization effects. Empirical absorption corrections were applied based on azimuthal ψ scans.

A crystal of **4** was mounted at the top of a quartz fiber using Apiezon grease, which was set on a Rigaku AFC7 equipped with a MSC/ADSC Quantum1 CCD detector. The measurements were made by using Mo–K_α radiation at -100°C under a cold nitrogen stream. The temperature was calibrated, before the data collection, by a thermocouple placed at the position where the crystal is to be mounted. After the crystal had been carefully centered at the X-ray beam, four preliminary data frames were measured at 0.5° increments of ω, in order to assess the crystal quality. Correction for high-energy background events in the images was made by collecting each data frame twice with 15 s exposure, and noncorrelating events were eliminated. A total of 197 reflections with $I > 6\sigma(I)$ were selected for calculations of a preliminary unit cell. The intensity images were measured at 0.5° intervals of ω for a duration of 50 s each. The frame data were integrated using the d*TREK program package, and an absorption correction was performed using the REQAB program. The 35300 integrated reflections were averaged in the point group 4/mmm to give 3014 unique reflections. Of these, 2488 reflections with $I > 3\sigma(\mathrm{I})$ were considered as observed.

All calculations were performed with the TEXSAN program package. The structures of **1**, **4**, and **5** were solved by direct methods, locating in all three cases the tungsten positions. The other atoms were found in subsequent Fourier maps, and then the structures were refined by full-matrix least squares. All non-hydrogen atoms were refined anisotropically, and the hydrogen atoms were located at calculated positions with the C–H distance of 0.97 Å. These crystallographic data are summarized in Table 3.

4. Supplementary material

Crystallographic data for the structural analyses have been deposited with the Cambridge Crystallographic Data Centre, CCDC no. 124953 for **1**, no. 124954 for **4**, and no. 124955 for **5**.

References

[1] (a) H. Kawaguchi, K. Yamada, J.-P. Lang, K. Tatsumi, J. Am. Chem. Soc. 119 (1997) 10346. (b) H. Kawaguchi, K. Tatsumi, J. Am. Chem. Soc. 117 (1995) 3885.
[2] S.-M. Koo, R. Bergero, A. Salifoglou, D. Coucouvanis, Inorg. Chem. 29 (1990) 4844.
[3] (a) J.R. Dilworth, R.L. Richards, P. Dahlstrom, J. Hutchinson, S. Kumar, J. Zubieta, J. Chem. Soc. Dalton. Trans. (1983) 1489. (b) J.L. Davidson, W.F. Wilson, K.W. Muir, J. Chem. Soc. Chem. Commun. (1985) 460. (c) N.M. Agh-Atabay, J.L. Davidson, G. Douglas, K.W. Muir, J. Chem. Soc. Chem. Commun. (1989) 549. (d) P.M. Boorman, M. Wang, M. Parvez, J. Chem. Soc. Chem. Commun. (1995) 999. (e) S. Thomas, P.J. Lim, R.W. Gable, C.G. Young, Inorg. Chem. 37 (1998) 590.
[4] W.A. Wan Abu Bakar, J.L. Davidson, W.E. Lindsell, K.J. McCullough, J. Chem. Soc. Dalton Trans. (1990) 61.
[5] M.L. Listemann, J.C. Dewan, R.R. Schrock, J. Am. Chem. Soc. 107 (1985) 7207.
[6] H. Brunner, R. Grabl, W. Meier, J. Wachter, B. Nuber, M.L. Ziegler, J. Organomet. Chem. 434 (1992) 63.
[7] M.S. Rau, C.M. Kretz, G.L. Geoffroy, A.L. Rheingold, Organometallics 12 (1993) 3447.
[8] H. Kawaguchi, K. Yamada, T. Komuro, K. Tatsumi, manuscript in preparation.
[9] A.C. Filippou, A.R. Dias, A.M. Martins, C.C. Romão, J. Organomet. Chem. 455 (1992) 129.
[10] (a) S.T. Krueger, R. Poli, A.L.A.L. Rheingold, D.L. Staley, Inorg. Chem. 28 (1989) 4599. (b) F. Abugideiri, D.W. Keogh, R. Poli, J. Chem. Soc. Chem. Commun. (1994) 2317.
[11] A.H. Liu, R.C. Murray, J.C. Dewan, B.D. Santarsiero, R.R. Schrock, J. Am. Chem. Soc. 109 (1987) 4282.